Available online at www.pelagiaresearchlibrary.com

Pelagia Research Library

Advances in Applied Science Research, 2012, 3 (2):1175-1184

ISSN: 0976-8610
CODEN (USA): AASRFC

Synthesis and Characterization of Local Impurities Doped Stannous Iodide (SnI_2) Crystal in Silica Gel

[1]Okpala V. Uche, [2]Ezema I. Felix and [2]Osuji U. Rose

[1]Department of Industrial Physics, Anambra State University, Uli, Anambra State
[2]Department of Physics and Astronomy, University of Nigeria, Nsukka, Nigeria

---

ABSTRACT

Crystals of un- doped and local impurities doped Stannous Iodide (SnI_2) were grown by sol gel technique. The optical properties of the materials were determined using a JENWAY 6405 UV-VIS spectrophotometer operating at a wavelength range of 200nm to 1200nm at an interval of 5nm. The crystallite size lies between 2.70 – 3.05 showing that they are polymer nano materials. The average refractive index (n) is between 0.6 and 2.9. The band gaps are from 3.2 to 4.3 showing that they are wide band gap materials and are good refractory materials.

Key words: Sol gel, Optical properties, Silica model and Local impurities.

INTRODUCTION

Stannous Iodide also known as tin (II) iodide (SnI_2) is an ionic compound of tin and iodine. It is a red- orange solid [1].

Dopants from local materials (Bamboo, Raffia, Potash).
The advancement in nanotechnology has called for the manipulation of the chemistry of materials. Nano technology is the engineering and fabrication of materials with structures smaller than 100nm or one tenth of a micron. A nano metre is one over one million or one thousandth of a micron. It is about the size of six carbon atoms aligned or 10 hydrogen atoms. It is also about 60,000 times smaller than the diameter of a human hair. In nano technology manufacturing we use either top–down or bottom-up [2]. Top-down manufacturing starts with bulk materials which are whittled down, until the features are left in nano scale. Bottom up manufacturing involves creating materials from individual atoms or molecules and then joining them together in a specific fashion. In this research work local dopants were produced using top-down approach.

Wood is largely made up of cellulose, which is in turn composed of repeating units of glucose, a simple sugar. Cellulose is composed of carbon, hydrogen and oxygen. When wood is burnt, the cellulose is oxidized to carbon dioxide and water. The remaining ashes contain a lot of elemental carbon in the form of soot. Soot is a colloidal carbon. It is in nano dimensions and has been used for centuries as pigments in inks, paints and as a reinforcing agent in rubber (tires) [2]. It is an approximate perfect black body and as such can be widely employed in solar energy technology. This has prompted us in this research work to consider locally produced dopant of about nanostructure to see how they permeate into the fabrics of said crystals.

(a) **Bamboo**
Bamboo is the most marvelous plant in nature. Bamboo is stronger than wood or timber in tension and compression. Chemical analysis reveals that bamboo has about 1.3% ash, 4.6% ethanol-toluene, 26.1% lignin, 49.7% cellulose, 27.7% pentosan [3]. In Hiroshima, Japan the only plant which survived the radiation of the atomic bomb in 1945 was a bamboo plant. In Costa Rica, a building made with bamboo withstood earthquake. It is used in many applications viz; in building it can be used as roof, floor, walls, scaffolds and supports in road construction as bridges. In power generation and agriculture as check dams in rivers, organic fertilizer, preservative medium. Its charcoal absorbs radiation like nuclear reactor etc.

(b) Raffia
The epidemis of the leaflet is the fiber and has been used to fabricate many ethnographical items [4]. Scanning electron microscopy revealed a layered structure: a top layer with a tile-like structure and a bottom layer with a honey comb-like structure. X-ray diffraction shows the presence of cellulose I_B with crystallinity index of 64%. The fiber density is 0.75+0.07, conferring to it the highest known specific mechanical properties among all vegetable fibers [5].

(c) Potash
Potash is a term coined by early American settlers who produced potassium carbonate by evaporating water filtered through wood ashes. The ash like crystalline residue remaining in the large iron pots was called 'potash' and was used in making soap. Potash (or carbonate of potash) is an impure form of potassium carbonate (K_2CO_3) mixed with other potassium salt. Potash has been used since antiquity in the manufacture of soap, glass and fertilizer [6]. Local potash is got by burning woods like tree fiber (ngu).

MATERIALS AND METHODS

Here, 25ml of sodium silicate solution of specific gravity 1.04 was titrated with some quantity of freshly prepared stannous chloride. The stannous chloride was prepared by dissolving it with few drops of concentrated hydrochloric acid to avoid hydrolysis and was diluted to the required strength. The essence of using freshly prepared stannous chloride was to avoid their oxidation. The gel formed after the titration was allowed to set, after which feed solutions of potassium iodide of varying concentration from 0.5 to 2.0N were added. After few hours, yellow whiskers of stannous iodide (SnI_2) were formed and a pipette drop of the impurity was added. The equation for the reaction is as written below,

$$SnCl_2 + 2KI \rightarrow SnI_2 + 2KCl \qquad (1.1)$$

$$2KI \rightarrow 2K^+ + 2I^- \qquad (1.2)\ [7]$$

Drying
The samples were first treated with all glass distilled water to avoid impurities and made slurry before it was introduced into a Buckner funnel covered with filter paper then attached to a suction flask connected to the vacuum pump through its nozzle. When the pump was put on it created a vacuum that allowed for the absorption of H_2O from the sample. The filter in the Buckner funnel prevented the solid from being sucked. The sample was the taken to the oven at an appropriate temperature of 104^0C for 30 minutes. After which it was placed inside the desiccators to maintain dryness. $CaCl_2$ was used as a desiccant.

RESULTS AND DISCUSSION

(a) Optical analysis
The optical studies for the sol gel grown crystals were done using a JENWAY 6405 UV- VIS spectrophotometer operating at a wavelength range of 200nm to 1200nm at intervals of 5nm. In the optical absorption study, deionised water was used as reference. The crystal samples were dissolved in deionised water forming a colloidal solution which was then subjected to UV-VIS analysis. The graphs of the optical analyses for the grown crystals of un-doped, doped Snl_2 and the impurities are shown in figures 1-12.

(i) Optical results for stannous iodide (SnI_2) and impurities.
In figure 1below, all the samples have high absorbance in the VIS region and decreased towards the NIR region.

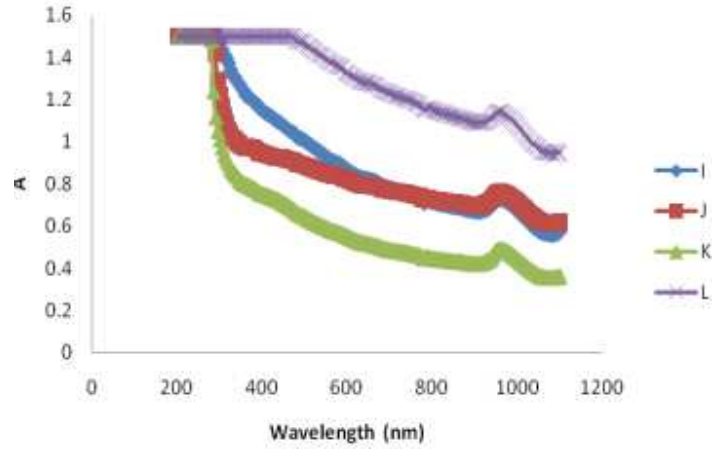

Figure 1: Absorbance (A) against Wavelength (nm) for SnI_2

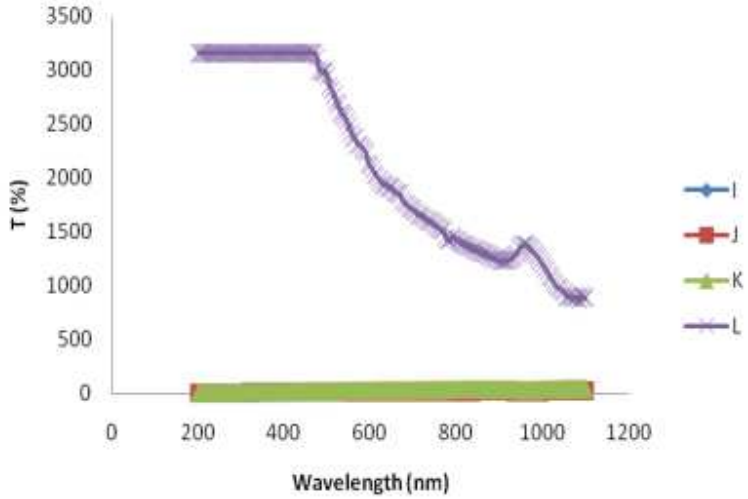

Figure 2: Transmittance (%) against Wavelength (nm) for SnI_2

In figure 2, samples I, J, K are not transmitting but L is highly transmitting from UV-VIS and decreased towards the NIR. Samples I, J, K are not reflecting but L has negative reflectance as seen in figure 3.

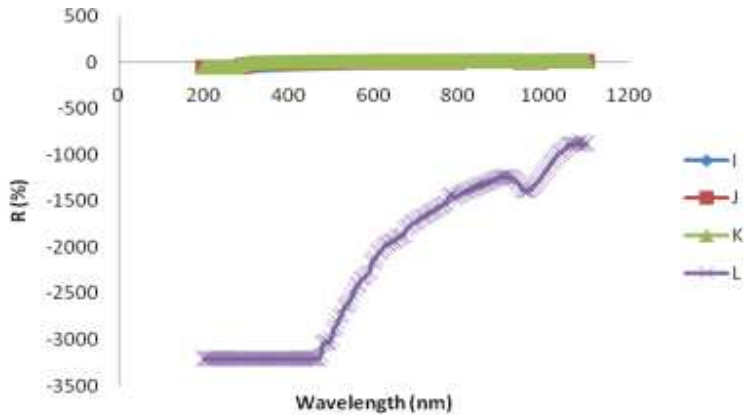

Figure 3: A plot of Reflectance (R) against wavelength (nm) for SnI_2.

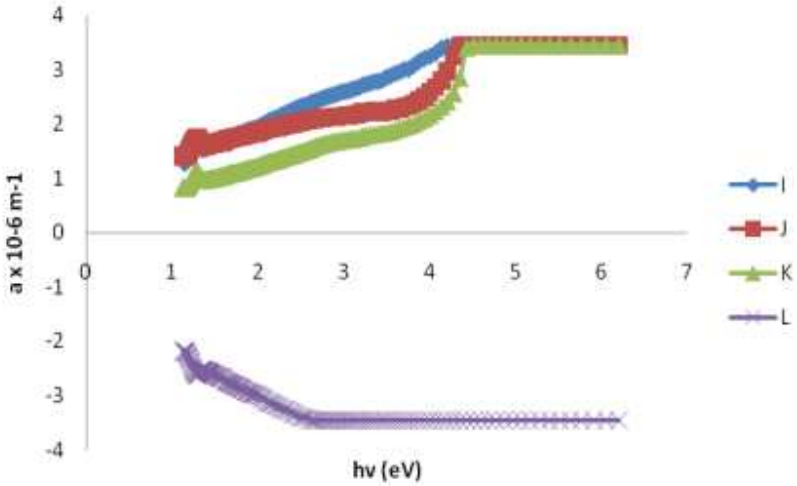

Figure 4: A plot of absorption coefficient (α) against photon energy (eV) for SnI_2.

In figure 4, samples I, J, K have absorption coefficient between 0.5 to 3.5 while sample L has negative absorption coefficient.

(ii) Results of optical band gaps for stannous iodide (SnI_2) and impurities.

In figure 5 below, the direct allowed $(ahυ)^2$ for I= 3.05, J= 3.6, K= 4.0 and L= 2.6 imply that the materials have wide band gaps and can be used in high temperature devices [8].

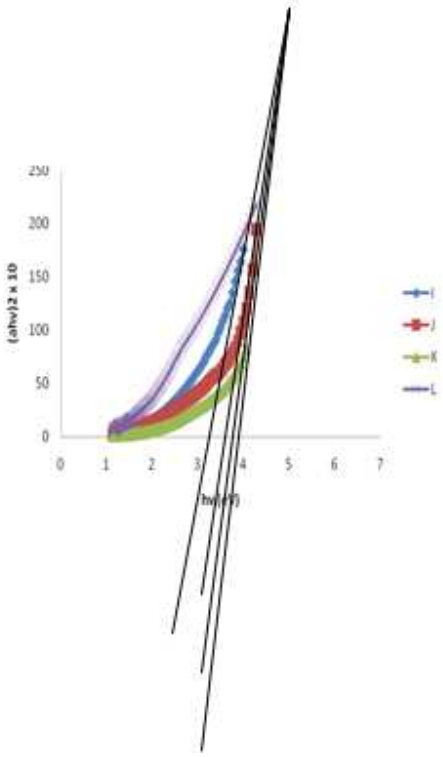

Figure 5: A plot of $(αhv)^2$ against photon energy (hv) for SnI_2

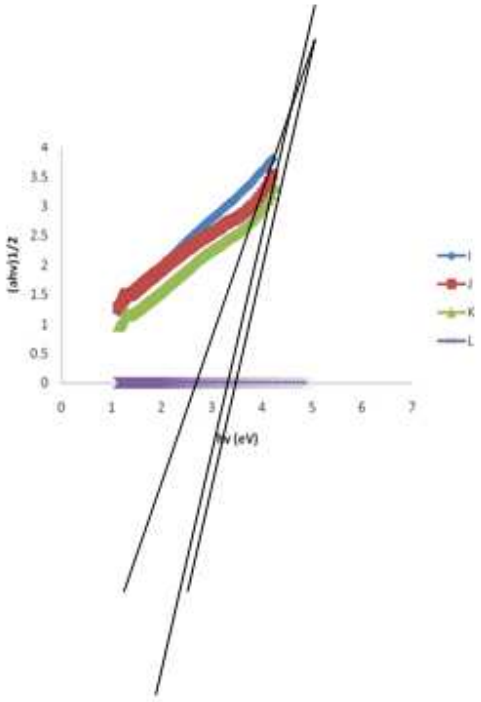

Figure 6: A plot of $(ahv)^{1/2}$ against photo energy (hv) for SnI_2.

From figure 6, the indirect allowed $(ah\upsilon)^{1/2}$ are I=2.2, J=3.5, K=3.9 and L=0, this show that samples I, J, K are wide band gap materials and can be used as refractory material [9] but L has no band gap.

In figure 7, samples I, J, K and L have indirect forbidden gap $(ah\upsilon)^{1/3}$ as 2.6, 3.05, 3.2 and 0 respectively.

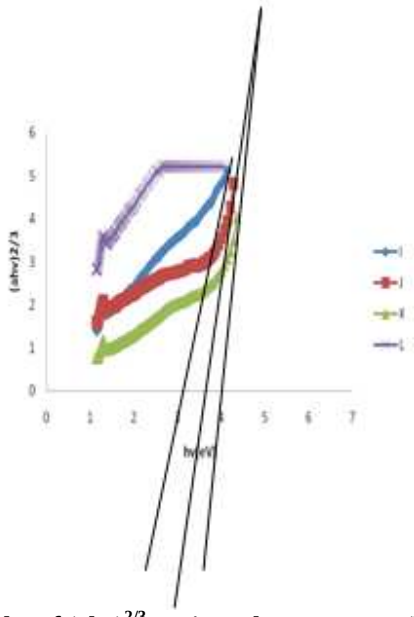

Figure 7: A plot of $(ahv)^{2/3}$ against photon energy (hv) for SnI_2

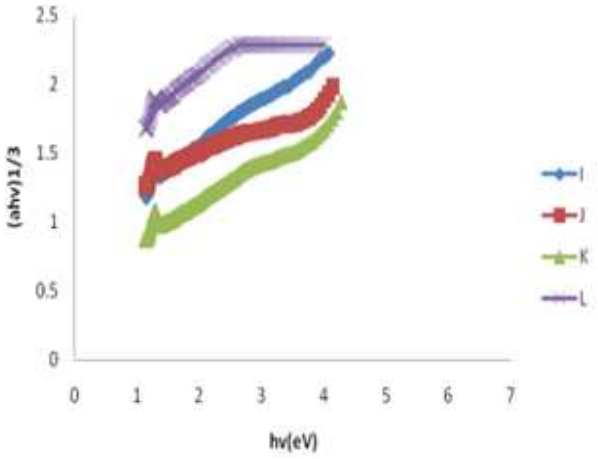

Figure 8: A plot of refractive index against (hv) for SnI_2.

Figure 8, shows that I=2.4, J=3.5, K=3.6 and L=0 this implies that the samples are wide direct forbidden gap $(ah\upsilon)^{2/3}$ materials but L has no band gap. From the results above, the band gaps lie between 2.2 and 3.9 which imply that the materials have wide band gaps except L which has direct, indirect allowed and direct allowed band gaps as O. Hence the materials can be employed as refractory materials that is in high power, high temperature, high frequency and short wavelength devices [8, 9].

(iii) Results of optical constants for stannous iodide (SnI_2) and impurities.
In figure 9, samples I, J, K and L have refractive indices between 0.6 to 2.4.

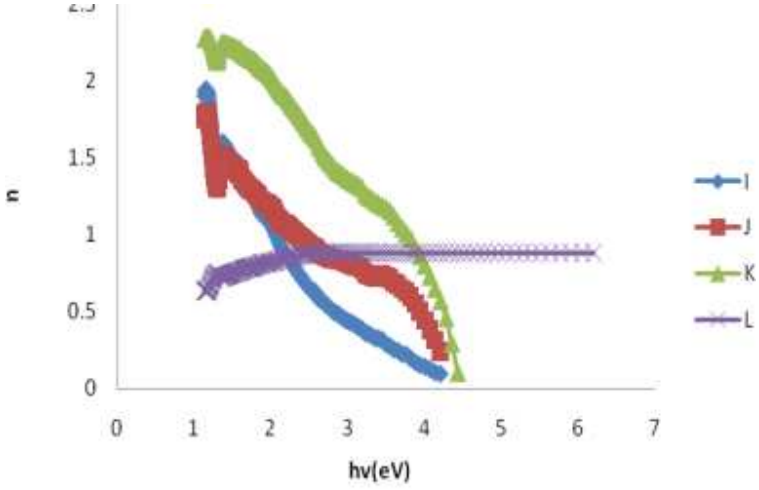

Figure 9: A plot of refractive index against (hv) for SnI_2.

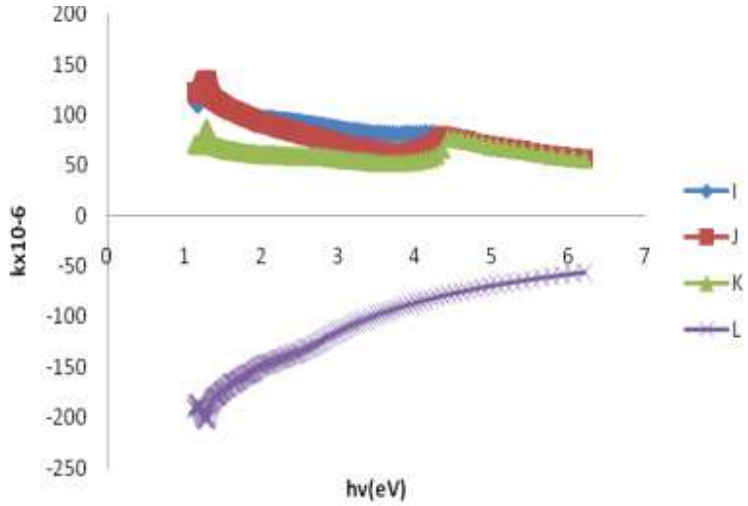

Figure 10: A plot of extinction coefficient (k) against photon energy (hv) for SnI_2

Samples I, J, K have extinction coefficient between 50 and 149 but L has negative extinction coefficient as seen in figure 10.

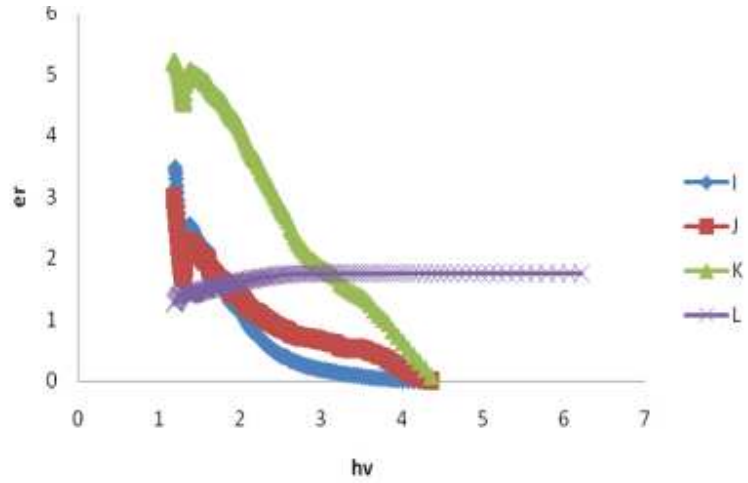

Figure 11: A plot of real dielectric (e_r) against photon energy (eV) for SnI_2

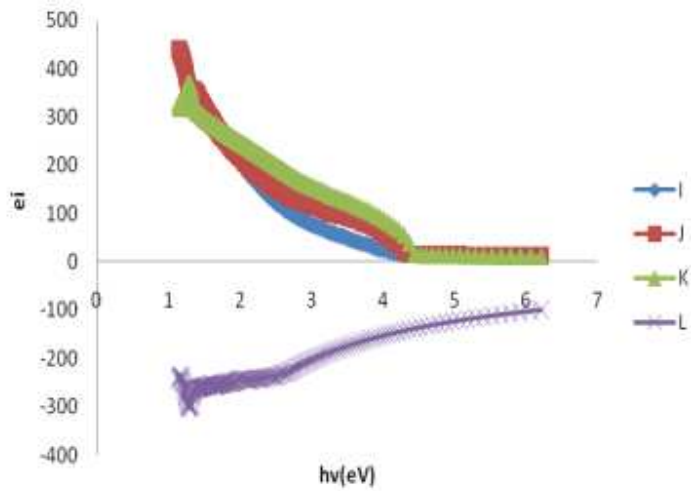

Figure 12: A plot of imaginary dielectric (e_i) against photon energy (hv) for SnI_2

In figure 11, sample K has the highest real dielectric and decreased towards zero. Samples J and I have real dielectrics between 0 and 3.2 but L has real dielectric as 1.2. In figure 12, samples I, J, K have imaginary dielectric between 0 and 480 and decreased to zero but sample L has negative imaginary dielectric.

Figures 13-16: XRD for Stannous Iodide (SnI_2)

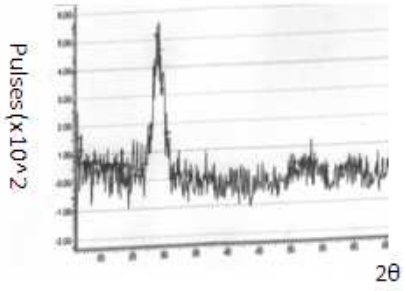

Figure 13: XRD spectra of un-doped SnI_2.

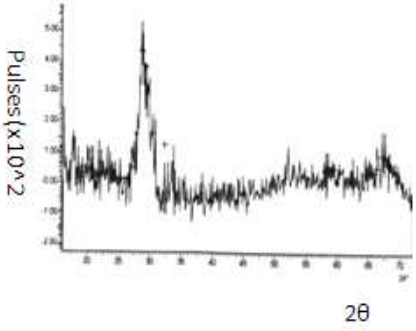

Figure 14: XRD spectra of potash doped SnI_2.

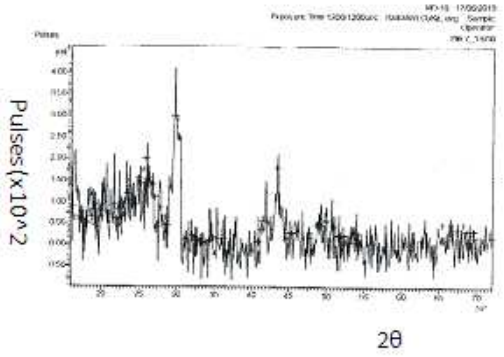

Figure 15: XRD spectra for bamboo doped SnI_2

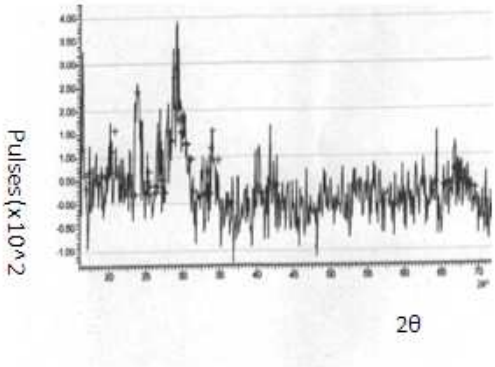

Figure 16: XRD spectra for raffia doped SnI_2

(b) Structural analysis

(i) X- Ray Diffraction (XRD).

X ray diffraction analysis (XRD) was used to uniquely identify the crystalline phases present in the crystals and to study the structural properties. The XRD characterization of the samples was carried out using MD-10 Diffractometer, which recorded diffractograms using CuK radiation. Diffraction patterns of the samples were recorded in the 2θ range from 10^o to 72^o. XRD spectra in the figures revealed that the compounds grown are crystalline in nature. For each spectrum, the crystallite size D, was determined using the Debye Scherer formula [10,11] as given below:

$D=K\lambda/ß\cos\theta$ …… (1.3) [10, 11]

Where K = 0.9 is the shape factor, λ= 1.5409Å, θ is the diffraction peak angle (Bragg's Angle) in degrees and ß is the corresponding diffraction peak. The XRD diffractograms for un-doped, impurity doped and the local dopants are shown on figures 13-16.

In figure 13, sample I has 2θ at 17.27, 22.07, 22.61 for stannous and 2θ at 14.79 for potassium tin oxide with peaks 110, 101, 020 and 011 respectively. In figure 14, sample J has 19.87 at 002 showing sodium 6 silicate ($Na_6Si_8O_{19}$), 21.14 at peak 011 shows sodium 2 silicate ($Na_2Si_2O_5$), 27.20 at 102 shows the presence of trydynite-20 (silicon oxide) and 28.59 at 100 showing KCl. In figure 15, sample K has 2θ at 17.30 and 25.85 showing the presence of sodium strontium phosphate ($NaSrPO_4$) and 2θ at 21.14 and 20.74 as Nitro silicate ($Na_2Si_2O_5$). In figure 16, L at 2θ is 20.26 is coesite, 2θ at 18.54 is sodium silicate ($Na_2Si_2O_5$), 2θ at 20.45 is potassium chlorate ($KClO_4$) and 2θ at 17.39 is potassium iron oxide (K_2FeO_4). The crystallite size of the materials lies between 2.70 – 3.05 implying that they are polymer nano materials and as such can be used in nano technology applications [10--20].

CONCLUSION

At this point we conclude that;

- Our results show that local materials from African environment can affect the optical and structural properties of semi conductor materials/ crystals [20].
- The presence of locally produced dopants have enabled us to grow hybrid compounds of binary, ternary and quaternary constitutions such as stannous iodide (SnI_2), sodium 6 silicate ($Na_6Si_8O_{19}$), sodium strontium phosphate ($NaSrPO_4$), potassium iron oxide (K_2FeO_4) that can be employed in solid state and materials industries.
- They are direct band gap materials with band gap from 3.1eV to 4.0eV, this shows that they are wide band gap semi conductors and can be employed in high power, high temperature, high frequency materials, optoelectronic devices and as heat sink, [20].
- The reduced particle size from 2.70nM to 3.05nM is a function of the broadness of the peaks and as such makes them good nano materials [15-20]]
- The sharpness of the peaks indicates that they are highly crystalline and as such are semiconductor materials that can be employed in solar energy applications [15-20].
- The broadness of the diffractogram shows that the materials are good for nano technology applications [20].

REFERENCES

[1] Chemistry Periodic Table: Tin Compound data- Tin II Iodide.
[2] Edwards S.E., Wenham: Wiley-VCH Verlag GMBH $ Co. KGA, **2006**, 1-5
[3] Baries, K., the Architecture of Simon Valez, Colombia, **2004**, 45.
[4] Elenga R.G., Dirias G.F., Maniongui J.G., Djemia P. and Biget M.P., Science Direct, **2008**, 3:31.
[5] Elenga R.G., Dirias, G.F., Maniongni J.G., Djemia P and Biget M.P., Science Direct, **2009**, 40:418.
[6] Nichol R.B., Potash and Phosphate Institute, **2008**, 78.
[7] Ochuenwike C.C., Unpublished M.Sc. Thesis, **1986**, 77-80.
[8] Yacobi B.G., New York: Kluwer Academic Publisher, **2004**, 148-151.
[9] Okpala U.V., *African Journal of Physics*, **2009**, 2: 114.
[10] Kondawar S.B., *Arch. Apl. Sci. Res.*, **2010**, 2(3) 225-230.
[11] Haung J.H. and Liu C.P., *Thin Solid Films*, **2006**, 498: 152-156.
[12] Pradha A.K., Hunter D., Zhang K., Dadson J.B., Mohanty S., Williams T.M., Lord K., Rakhiimov R.R., Roy U.N., Cui Y., Burger A., Zhang. and Sellmyer D.J., *Applied Surface Science*, **2005**, 252: 1628-1633.

[13] Amma B.S., Ramakrishna K., Pattabi M., *Materials Chemistry and Physics*, **2005** 112: 789-792.
[14] Chahal R. P., Mahendia S., Tomar A.K. and Kuma S., *Chalcogenide Letters*, **2010** 7(8) 569-575.
[15] Santosh T.M. Pandurang C. P., Shrishail S. K. , Vikram S. K., and Lalasaheb P. D., *Adv. Appl. Sci. Res.*, **2011**, 2(5)9.
[16] Suresh K. B., Padmarkar A. S. and Suresh T. P., *Adv. Appl. Sci. Res.*, **2010**, 1(1) 29.
[17] Amrut S. L., Satish J.S., Ramchandra B. P. and Raghumani S. N., *Adv. Appl. Sci. Res.*, **2010**, 1 (2) 38.
[18] Hemant M., Balbir S. K. and Rajeev J., *Adv. Appl. Sci. Res.*, **2010,** 1(3)62
[19] Kaviyarasu K. and Prem A. D., *Adv. Appl. Sci. Res.*, **2011**, 2(6)133
[20] Okpala U.V., Ezema F.I. and Osuji R.U., *Adv. Appl. Sci. Res.*, **2012**, 3 (1) 103-109